On the Characterization of Sodium Alginate/ Gelatine-Based Hydrogels for Wound Dressing

Amarjargal Saarai,[1,2] Tomas Sedlacek,[1,2] Vera Kasparkova,[2,3] Takeshi Kitano,[1,2] Petr Saha[1,2]

[1]*Centre of Polymer Systems, University Institute, Tomas Bata University in Zlin, Nad Ovcirnou 3685, Zlin 760 01, Czech Republic*
[2]*Polymer Centre, Faculty of Technology, Tomas Bata University in Zlin, nam. T. G. Masaryka 275, Zlin 760 01, Czech Republic*
[3]*Department of Fat, Surfactant and Cosmetics Technology, Faculty of Technology, Tomas Bata University in Zlin, nam. T.G. Masaryka 5555, Zlin 760 01, Czech Republic*

Received 26 October 2011; accepted 26 November 2011
DOI 10.1002/app.36590
Published online in Wiley Online Library (wileyonlinelibrary.com).

ABSTRACT: In this study, sodium alginate/gelatine (SA/G) hydrogels were prepared to obtain wound dressing with good, moist, healing, and biocompatibility properties. The physicochemical properties of hydrogels were evaluated by scanning electron microscopy, Fourier transform infrared spectroscopy, and a swelling test. Dynamic viscoelastic properties including the storage, loss moduli, G' and G'', and loss angle, tan delta of both freshly prepared and swelled gels were examined in oscillatory experiments. Its results revealed that tested SA/G hydrogels exhibit highly elastic behavior similar to the viscoelastic response of human skin. Based on the performed analysis, it could be suggested that the SA/G hydrogel is a potential wound dressing material providing and maintaining the adequate moist environment required to prevent scab formation and the dehydration of the wound bed. © 2012 Wiley Periodicals, Inc. J Appl Polym Sci 000: 000–000, 2012

Key words: sodium alginate; gelatine; hydrogels; wound dressing; swelling behavior; viscoelastic properties

INTRODUCTION

The expansion of comprehensive medical and pharmaceutical wound care has led to considerable attention being placed on the development of wound dressing materials. The ideal dressing material needs to ensure that the wound remains free of infection and moist with exudates but not macerated, while also fulfilling prerequisites concerning structure and biocompatibility. In addition, it should permit the exchange of gases, maintain an impermeable layer to microorganisms so as to prevent secondary infection, not inflame any allergic reaction through prolonged contact with tissue, and it should be removed without trauma and pain. Furthermore, the dressing must be physically strong even when wet, and easy to dispose of when removed.[1–8] Currently, there are numerous wound dressing materials with different functions (e.g., antibacterial, absorbent, adherence, and debridement) and physical forms (e.g., film, foam, gel) as well as materials (e.g. carrageenan, alginate, collagen). Among these materials, hydrogels based on polymeric and biopolymeric materials forming a three-dimensional network, are considered as promising options because of their insoluble, swellable, and hydrophilic properties. Moreover, they can be fabricated to be flexible, durable, and permeable to water vapour and metabolites while also safely covering the wound to prevent bacterial infection. Due to these advantages, hydrogels possess most of the desirable characteristics of an ideal dressing.

Alginates belong to a group of the extensively studied and commonly used gel-forming agents, composed of rather stiff linear polysaccharides. They are obtained by extraction from seaweed, where they occur naturally as mixed calcium and sodium salts of alginic acid consisting mainly of residues of β-1,4-linked D-mannuronic acid and α-1,4-linked L-glucuronic acid. On absorbing moisture, gluronic acid forms firmer gels while mannuronate acid is able to form soft, flexible gels.[8–10] The use of alginate-based hydrogels as dressing can be attributed to their ability to form gels on contact with moisture. Their high moisture absorption occurs via the formation of a strong hydrophilic gel, which limits wound secretions and minimizes bacterial contamination.[4,11] Sodium alginate (SA) used as a wound dressing

Correspondence to: A. Saarai (amarjargal_sa@yahoo.com).
Contract grant sponsor: Ministry of Education, Youth and Sports of the Czech Republic; contract grant number: MSM 70088352101.
Contract grant sponsor: Ministry of Industry and Trade of the Czech Republic; contract grant number: project 2A-1TP1/126.

meets the requirements of nontoxicity and a high level of exudation absorbency.[12,13]

Gelatine (G), another natural polymer, is a collagen-derived connective tissue protein with unique gelation properties attributed to a physical crosslinking of the triple-helix conformation of native collagen.[14–17] It can be obtained either from acidic (Type A gelatine) or alkaline hydrolysis (Type B gelatine) collagen. Type B has more carboxyl groups and a lower isoelectric point (IEP-4.8-5.0) than Type A (IEP-7.0-9.0).[17–19] Gelatine has been used in a wide variety of wound dressings because of its high water absorption and ability to activate microphages and haemostasis in bleeding wounds.[20,21] The main feature of gelatine is its ability to form a thermally reversible network in aqueous media.[17,22] The structural network in gelatine-based hydrogels is a combination of elastic, triple-helix conformation, and a viscous chain, disorder of polypeptide fragment, units.[14,17,23]

The preparation and use of hydrogels based on a combination of either SA or gelatine with other natural or synthetic polymers (agar/SA,[24] chitosan/SA,[25] SA/poly(γ-glutamic acid),[26] polyvinyl alcohol/SA,[11] chitosan/gelatine,[27] polyvinyl alcohol/gelatine,[20] oxidized hyaluronan/gelatine,[28] gelatine/hyaluronate[29] etc.) as wound dressings is being widely reported, while it is referred that these hydrogels posses a good biocompatibility and fulfil the required quality criteria for wound dressing material. However, the combination of SA and gelatine (G) within the list of commercial products of hydrogels for health care applications, especially for wound treatment or wound protection was studied sporadically.[29,30]

The interest in hydrogels is also motivated by their soft consistency derived from their high water content and their tissue-like behavior caused by their specific viscoelastic performance.[31] These viscoelastic properties are strictly related to the internal structure of hydrogels in terms of, e.g., crosslinking density, chain length, degree of swelling, and molecule stiffness of the used polymer. Optimized viscoelastic properties, such as storage (G') and loss modulus (G''), investigated using dynamic mechanical analysis (DMA) and rheometric analysis,[32] are of concern during hydrogel properties development and help to meet the requirements for its absorption efficacy, elasticity as well as painless removal.[33,34]

However, so far there are only a few reports concerning DMA and/or rheometric analyses of wound dressing hydrogels. The use of these methods for investigation of hydrogel viscoelastic behavior is often complicated by compositional and swelling changes[35–37] as well as structural defects in the gel network.[38,39] Meyvis et al.[32] compared the use of DMA (multi-strain and single strain) and oscillatory shear rheometry for the characterization of pharmaceutical hydrogels. They reported that the choice of method for the mechanical characterization of hydrogels depends on the accuracy, speed of measurement, and the amount of sample available. The best agreement was found between the "multi- strain" DMA and rheometer results. In their review, Anseth et al.,[37] thoroughly resolved the mechanical properties of polymer-based hydrogels using tensile and DMA tests in dependence on monomers used, polymerization conditions and effect of degree of swelling. They reported that the mechanical properties are highly dependent on polymer structure, especially the crosslinking density and the degree of swelling.

For this study, "SA/G hydrogels" with various concentrations of SA and gelatine were prepared with the aim to obtain and characterize blends of SA and G as a reference system suitable for highly hydrophilic and biocompatible wound dressings and other medical applications. Desirable properties of SA and gelatine were the motivation behind the choice of these natural materials and were prioritized over the fact that physically crosslinked gelatine-based hydrogels are known to dissolve as they are immersed in physiological buffer saline or water at intended service temperature (above 35°C). Blended hydrogels having increase insolubility will be objective of future work utilizing crosslinking of either G, or SA via glutaraldehyde, and $CaCl_2$, respectively.

The viscoelastic properties of SA/G hydrogels were studied using an oscillatory shear rheological analysis and correlated to the various compositions of the hydrogels. Scanning electron microscopy (SEM), Fourier transform infrared (FTIR) spectroscopy, and a swelling and viscoelastic technique were utilized for the study of the prepared materials.

MATERIALS AND METHODS

Materials

SA, gelatine (Type B, 250 bloom), glycerol, and sodium chloride (NaCl) (analytical grade) were obtained from Lachema (Czech Republic). Polyethylene glycol (PEG, MW: 3000 g/mol) was purchased from Sigma (Czech Republic). Reverse osmosis purified water was used for the hydrogel preparation and swelling measurements.

Preparation of SA/G hydrogels

The "SA/G hydrogels" were prepared using various concentrations of SA and G while keeping the amount of other components (PEG, glycerol, NaCI and water) constant. An aqueous gelatine solution of (15–30% w/w) was prepared by dissolving polymer

TABLE I
Composition of the SA/G Hydrogels

Hydrogel composition SA/G (g)	70/30	60/40	50/50	40/60	30/70
Gelatine (G)	3	4	5	6	7
Sodium alginate (SA)	7	6	5	4	3
Poly ethylene glycol (PEG)	2	2	2	2	2
Glycerol	2	2	2	2	2
Sodium chloride (NaCl)	0.2	0.2	0.2	0.2	0.2
Water	20	20	20	20	20

granules in water at 80°C under continuous stirring (300 rpm) until a homogeneous solution was obtained. After dissolving G, relevant portions of SA, PEG, NaCl and glycerol (see Table I) were added. Then, the stirring rate was reduced to 100 rpm and continued at 80°C for another 5 min until a viscous hydrogel was formed. The prepared hydrogel was poured into circular moulds (diameter 25 mm) with a thickness of 2 mm and cooled down (samples denoted "A"). Finally, the samples were dried (samples denoted "B") at room temperature for 72 h. For purpose of comparison, reference samples composed of pure G and pure SA were prepared using the identical procedure.

Scanning electron microscopy

The cross-sectional morphologies of the SA/G hydrogels were examined by SEM at an accelerating voltage of 20 kV (VEGA\\LMU, TESCAN, Czech Republic). Cross-sectional specimens were prepared by fracturing of B samples in liquid nitrogen to examine miscibility and morphology of the blended, dried systems preceding swelling phase. Before observation, the specimens were coated with a thin layer of gold under a vacuum. SEM images were analyzed using an image analysis VEGA Software.

Swelling behavior

The SA/G hydrogels were immersed in distilled water (pH 7.0) at room temperature (23 ± 2°C). The degree of swelling was determined gravimetrically. The swelled samples (denoted C) were taken from the water at selected time intervals (1, 2, 3, 4, 8, 12 h), wiped with tissue paper, weighed and placed in water again. The percentage of swelling and water content were calculated using the following equation:

$$\text{Swelling}\,\% = \frac{(W_S - W_D)}{W_D} \times 100 \quad (1)$$

$$\text{Water content}\,\% = \frac{(W_S - W_D)}{W_S} \times 100 \quad (2)$$

where W_S and W_D are the weights of the swollen and dry samples, respectively.

Viscoelastic properties

The viscoelastic properties of the SA/G hydrogels were measured by rotational rheometer (Rheometrics ARES Rheometer, TA Instruments) using a parallel-plate 25 mm in diameter. All measurements were performed in the linear viscoelastic regime with a strain of 1%. The measurement went through frequency scanning at 33°C (surface temperature of human skin[40]) in the frequency range of 0.1–100 rad/s. The storage modulus (G'), loss modulus (G''), complex viscosity (η^*), and tan delta ($\delta = G''/G'$) of the samples were recorded as a function of frequency. Each measurement was performed at least twice, on two different disk specimens from the same hydrogel sample.

Fourier transform infrared spectroscopy

The chemical composition of the samples B was investigated by FTIR spectroscopy. Attenuated total reflectance/Fourier transform infrared (ATR–FTIR) spectroscopy was conducted with a FTIR instrument (Nicolet 320, Nicolet Instrument Corporation) using a Zn-Se crystal and the software package OMNIC over the range of 4000–1000 cm^{-1}. A resolution of 2 cm^{-1} was maintained in all cases.

RESULTS AND DISCUSSION

Morphology of SA/G hydrogels

The effects of SA and G contents on the morphology of dried SA/G hydrogels (sample B) are shown in SEM micrographs in Figure 1. The morphologies of SA/G 100/0 and SA/G 0/100 are depicted in Figure 1(a,b), respectively. From the figures, it is seen that the pure SA sample shows a particle-like, aggregate structure while the pure G sample exhibits uniform, relatively homogenous morphology.

The morphologies of SA/G hydrogel materials of various compositions (70/30, 60/40, 50/50, 40/60, and 30/70) are shown in Figure 1(c–g), respectively. By comparison, it is obvious that the morphologies of the pure samples differ significantly from the binary blends. The morphologies of the SA/G-70/30, 60/40, and 50/50 samples reveal structures having

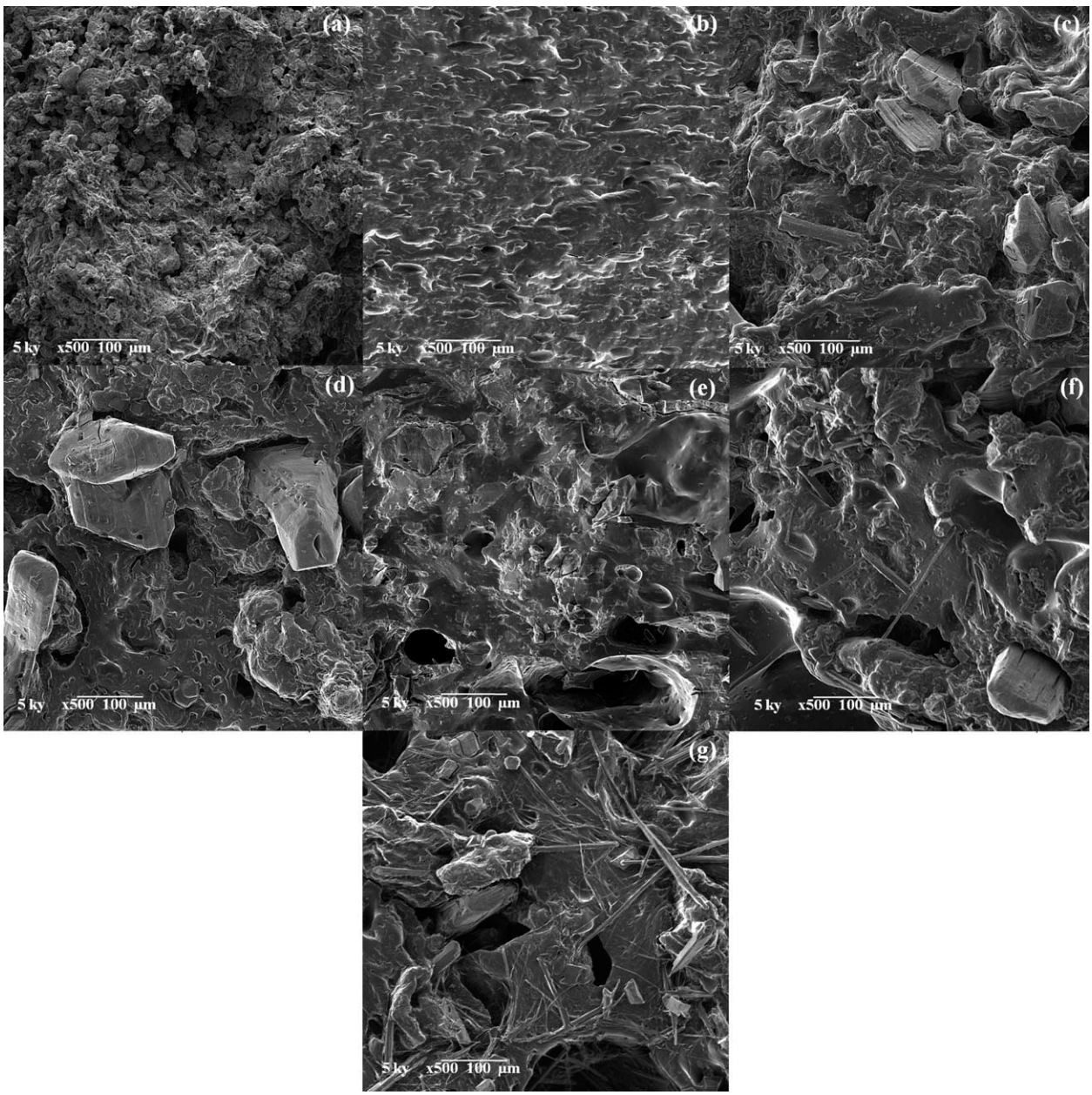

Figure 1 SEM micrographs of dried hydrogels: (a) SA/G-100/0, (b) SA/G-0/100, (c) SA/G-70/30, (d) SA/G-60/40, (e) SA/G-50/50, (f) SA/G-40/60, and (g) SA/G-30/70.

uniform SA as a matrix and G as dispersed phase [Fig. 1(c–e)]. On the other hand, samples with a prevailing amount of G, SA/G 40/60 and 30/70, have G as the matrix and SA as the dispersed phase [Fig. 1(f,g)]. It should be noted that for the samples with SA as the matrix, a droplet-like morphology of minor G phase is observed, while samples with G as the matrix render a fibrous morphology of SA phase.

Swelling behavior of G/SA hydrogels

The degree of swelling indicates the ability of the dressing to absorb the wound fluid and exudates. The swelling behavior of SA/G hydrogels as a function of time is shown in Figure 2. As can be seen, all samples demonstrate a rapid increase in swelling degree within the first 4 h, and this swelling continues to increase slowly for up to 12 h (Table II). However, within the tested time interval, only the samples with lower G content reach the equilibrium swelling. It is furthermore obvious that swelling degree decreases with an increase of SA content in the hydrogels, which can be attributed to the structure of the SA matrix, with pores of small sizes hindering the diffusion of water molecules into the hydrogel structure. A similar behavior for SA-based hydrogels has been reported by Bajpai et al.[41] and Anmika

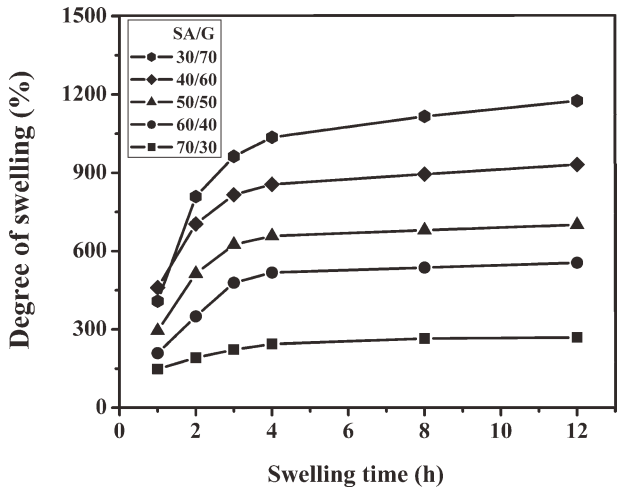

Figure 2 Effect of composition and time on the degree of swelling.

et al.[42] The increase in the swelling degree of hydrogel samples with high G content refers to the strong hydrophilicity of G molecules, which is reportedly due to the presence of an ionizable NH_2^- and COO^- functional group that can increase the volume between polymeric chains and the swelling capacity of the hydrogel by hydrostatic repulsion.[41,43]

A maximum swelling degree of SA/G hydrogels at 1176% was observed in the composition SA/G 30/70. Even such a level of swelling is not a final value and would be slightly higher when approaching equilibrium state. Analogous swelling behaviors were observed for the commercial hydrogel dressings Geliperm® (Geistilich, Switzerland) and Vigilon® (Bard, Crawley, UK).[21,30] As to water uptake, the maximum water content of all swelled hydrogels (Samples C) was in the range of 74–94% (Table II), indicating that the SA/G hydrogels could fulfil the requirement of an ideal wound dressing[1–3,21,44] and prevent a wound from accumulation of fluid by absorbing the exudates.

Viscoelastic properties of G/SA hydrogels

The angular frequency dependence of the storage modulus (G') and loss modulus (G'') for SA/G hydrogels is depicted in Figure 3. From Figure 3(a) it can be seen that the G' of all hydrogels is almost one order of magnitude higher than G'' over the whole angular frequency range and both the G' and G'' of all samples slightly increase with angular frequency. In addition, an increase in G' and G'' values is observed when the SA concentration rises, probably due to the increased number of SA chains that produce a dense network.[41,45] Obviously, after 8 h swelling, the G' and G'' of all samples drop dramatically because of the presence of water, which increases mobility of the gel network and decreases stiffness [Fig. 3(b)]. It should be noted that the described viscoelastic behavior of swelled SA/G hydrogels is in agreement with the viscoelastic response of human skin reported in the literature.[46,47]

In Figure 4(a), the tan δ of samples A is plotted against angular frequency. At first, a plateau is observed until 5 rad/s, then an increasing trend, due to the enhanced influence of the viscous part, attended by a more significant change in G'' compare with G', begins. The angular frequency dependency of the tan δ values for swelled samples C is shown in Figure 4(b). Over the whole frequency range tan δ gently increases, along with a slightly steeper increase of G'' with the frequency than that of G' [see Fig. 4(a)]. Interestingly, the SA/G 70/30

TABLE II
Physical Characteristics of the SA/G Hydrogel Samples

Hydrogel composition SA/G	70/30	60/40	50/50	40/60	30/70	Image of hydrogels
Samples after preparation A (before drying), $n = 3$						
Weight (g)	0.735 ± 0.064	0.729 ± 0.051	0.894 ± 0.117	0.858 ± 0.161	0.876 ± 0.094	
Diameter (mm)	25.0 ± 0.00	25.0 ± 0.00	25.0 ± 0.00	25.0 ± 0.00	25.0 ± 0.00	
Thickness (mm)	1.94 ± 0.23	1.74 ± 0.18	1.99 ± 0.21	1.70 ± 0.33	1.76 ± 0.25	
Moisture content (%)	49.2 ± 0.52	46.9 ± 0.76	49.4 ± 0.17	49.1 ± 1.24	52.9 ± 0.86	
Dried samples B (after drying), $n = 3$						
Weight (g)	0.373 ± 0.032	0.386 ± 0.027	0.452 ± 0.059	0.452 ± 0.082	0.412 ± 0.046	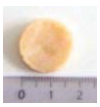
Diameter (mm)	19.82 ± 0.40	20.25 ± 0.54	20.71 ± 0.26	19.96 ± 0.14	20.92 ± 0.56	
Thickness (mm)	1.54 ± 0.19	1.23 ± 0.12	1.39 ± 0.19	1.19 ± 0.22	1.02 ± 0.16	
Swelled samples C (12 h after swelling), $n = 3$						
Weight (g)	1.387 ± 0.201	2.285 ± 0.47	2.295 ± 0.64	3.804 ± 0.81	3.981 ± 0.92	
Diameter (mm)	31 ± 2.14	38 ± 3.69	38.583 ± 3.6	42.21 ± 2.49	43.42 ± 3.87	
Thickness (mm)	2.29 ± 0.31	2.48 ± 0.198	2.55 ± 0.32	2.83 ± 0.49	2.90 ± 0.42	
Water content (%)	72.54 ± 4.68	81.86 ± 6.53	84.03 ± 3.96	87.97 ± 3.46	90.1 ± 3.74	

All measurements were done in triplicate.

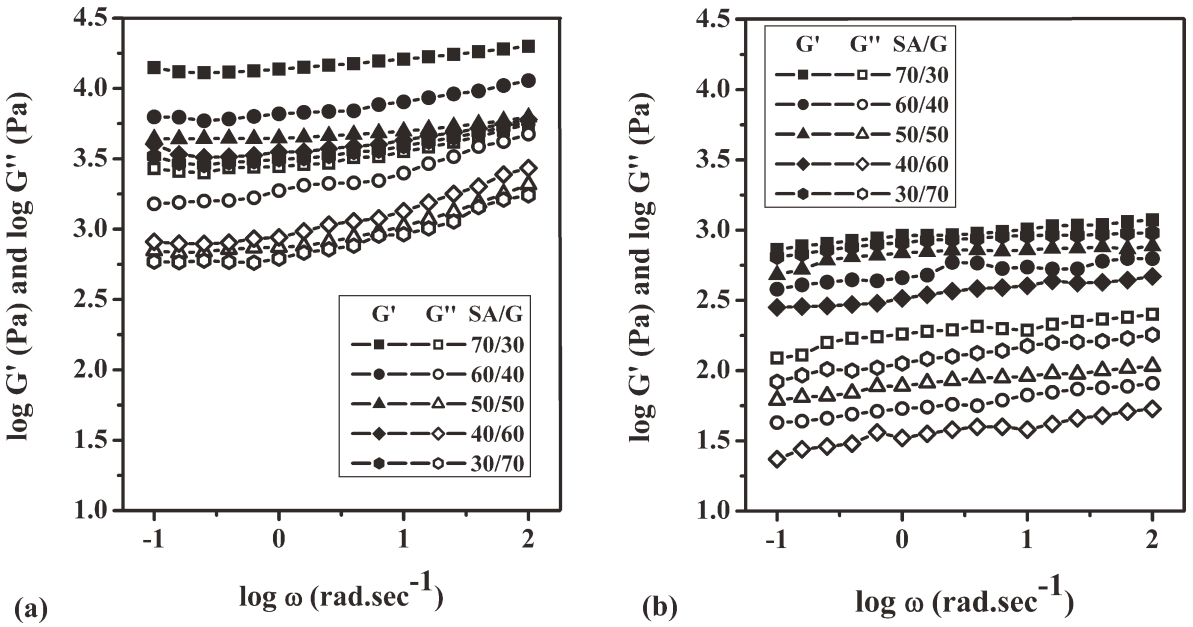

Figure 3 Storage, G', and Loss, G'', moduli of freshly prepared samples A (a) and 8 h swelled samples C (b).

and 30/70 samples are slightly more elastic than the other samples, most probably due to the different morphologies of the prepared hydrogels.

In Figure 5, the dependence of G' and G'' on the swelling time of the hydrogels with different ratios of SA/G at the angular frequency ω of 0.39 rad s^{-1} is shown. The viscoelastic moduli gradually decrease for up to 4 h swelling time. After this time period elapses, changes of G' and G'' are not so prominent. This observation complies with the swelling behavior depicted in Figure 2 describing the effect of composition and time on the degree of swelling.

The G' and G'' of samples A and C with different compositions, recorded at the angular frequency of 0.39, 3.9 and 39 rad s^{-1}, are depicted in Figure 6. Comparing samples A and C, it is obvious that after 8 h of swelling both G' and G'' drop notably; interestingly G'' undergoes a more significant change. Furthermore, as can be seen from Figure 6(a), both G' and G'' of samples A decrease with the increasing contents of G. The swelled samples C, contrary to the freshly prepared samples A, do not follow the same decreasing tendency of the storage and loss moduli with G content increase [Fig. 6(b)]. The maximum values of moduli for samples C were found in the compositions SA/G 70/30 and 30/70. The viscoelastic properties of these hydrogels are influenced by stiff molecules of SA representing either the

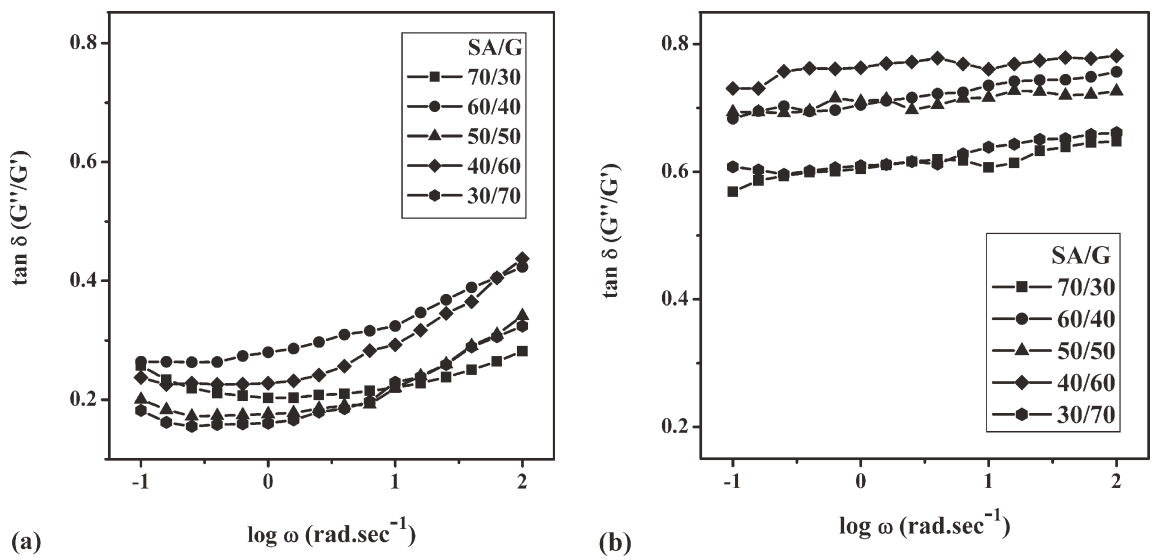

Figure 4 Effect of angular frequency on tan δ of samples A (a) and C (b).

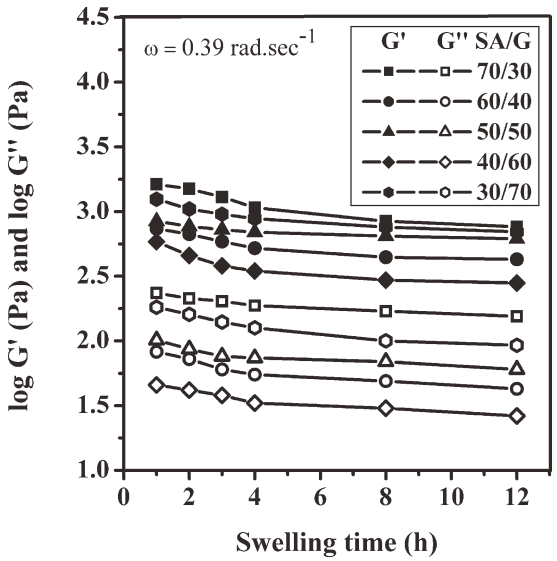

Figure 5 Effect of swelling time on storage modulus, G', and loss modulus, G'', of SA/G hydrogels.

continuous phase (SA/G 70/30) or needle-like dispersed particles (SA/G 30/70) in hydrogel structure. The local minimum of G' and G'' was observed for hydrogel compositions of SA/G 60/40 and 40/60. The authors believe that such behavior could be caused by phase separation phenomenon. Using SEM, it was determined that the morphology of 60/40 and 40/60 compositions induced specific porosity levels in a continuous phase matrix (SA/G 60/40) or in discontinuous phase particles (SA/G 40/60). Interestingly, viscoelastic moduli of G/SA 50/50 are higher than those of 40/60 and 60/40 at measured angular frequencies. This can be a consequence of attraction forces between the charged ions leading to intensive interactions by the balanced anionic carboxylate groups (—COO^-) of SA and the cationic protonated amino groups (NH_3^+) of gelatine.[48]

Figure 7 presents the relation between complex viscosity, η*, and angular frequency for samples C with various SA/G compositions and shows that η* decreases linearly with angular frequency. Furthermore, decreased η* of samples C have a similar trend as observed for G' and G'' [Fig. 6(b)].

The storage and loss moduli of samples C as a function of the swelling degree are represented in Figure 8(a,b). As can be seen in Figure 8(a), the highest values of G' are observed for the hydrogel of SA/G 70/30 composition. Notably, for this hydrogel the smallest change of swelling degree (200–300%) was connected with the most significant decline of storage modulus. On the other side, only a minor G' change over the widest region of swelling degree (400–1200%) was determined for the hydrogel with the opposite SA/G ratio of 30/70. The changes of swelling degree as well as changes of G' ($\Delta G''$) observed for samples with the composition of SA/G 60/40, 50/50, and 40/60 lie between the above mentioned SA/G 30/70 and 70/30 hydrogels. Furthermore, from Figure 8(a) it is clear that while the highest G' of unswelled samples was found for SA/G 70/30, the highest G' values of fully swelled hydrogels were recorded simultaneously for SA/G 70/30 and SA/G 30/70 samples.

Values of G'' for all studied samples are almost an order of magnitude lower than those of G' over the entire range of swelling [see Fig. 8(b)]. The results also reveal that the levels of G'' follow the trend described for G'. However, the magnitude of G'' changes ($\Delta G''$) is independent of hydrogel

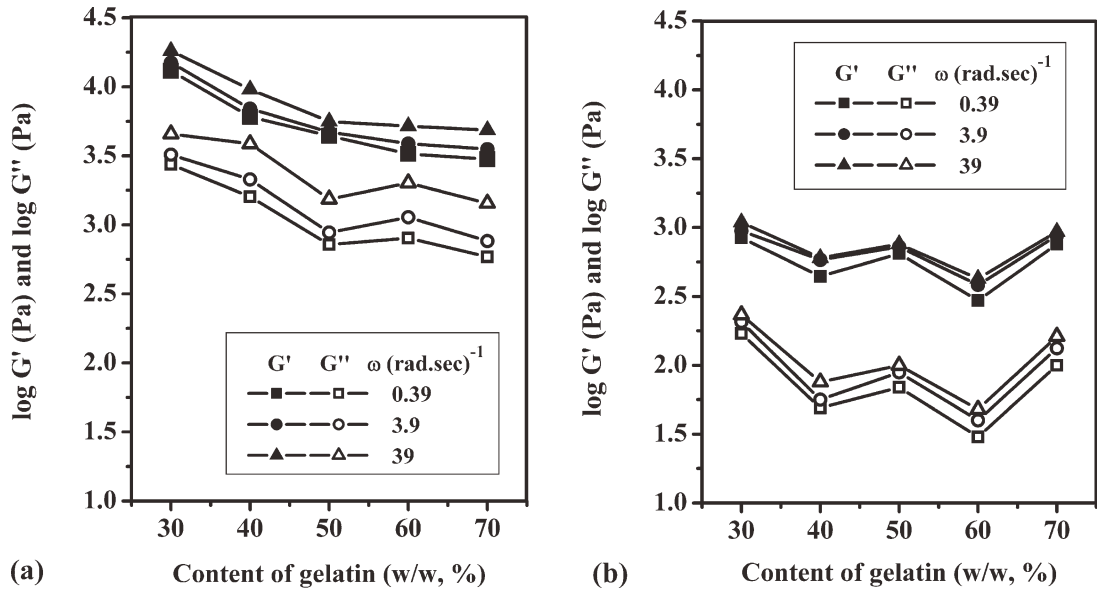

Figure 6 The effect of composition on storage modulus, G', and loss modulus, G'', of samples A (a) and samples C (b).

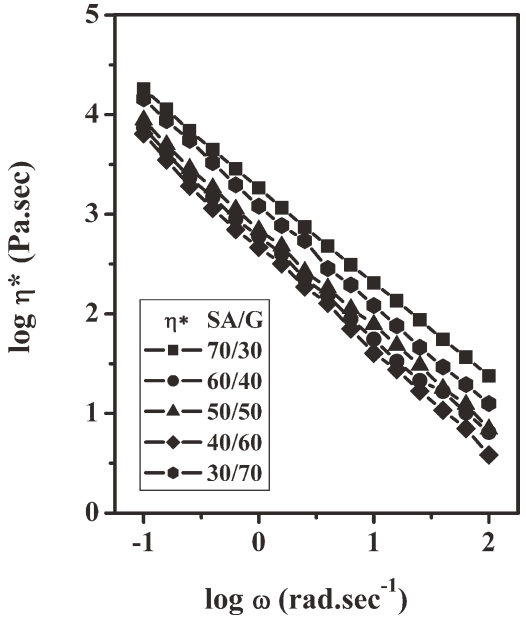

Figure 7 Effect of angular frequency on complex viscosity of samples C.

composition, thus differing significantly from the behavior of G' and indicating predominant elastic response within the course of hydrogel swelling.

The described results, namely the values of elastic (G') and viscous (G'') moduli and the swelling degrees of the prepared samples, indicate that the viscoelastic properties of SA/G hydrogels are appropriate for wound dressing.[49,50]

FTIR characterization of SA/G hydrogels

The FTIR spectra of G/SA hydrogels are shown in Figure 9. The FTIR spectrum of SA/G-100/0 indicates the characteristic absorption peaks observed at 3274 cm^{-1} typical for hydroxyl stretching and a peak at 1637 cm^{-1} which corresponds to a stretch of C=O. Peaks at 1521, 1458, 1408, and 1349 cm^{-1} in the SA spectrum indicate the anti-symmetric stretch and symmetric stretch of $-COO^-$ in associated carboxylic acid salt.[51,52] Two other interactions in the C—O stretch of C—OH groups can be found at 1030, 1080 cm^{-1} and the peak at 1248 cm^{-1} corresponds to the anti-symmetric stretching of C—O—C.

The FTIR spectrum of SA/G 0/100 exhibits a peak at 3309 cm^{-1} due to the N—H stretching in secondary amides, the C=O stretching at 1631 cm^{-1} for the amide I, which is characteristic of the coil structure of gelatine,[22] as well as N—H deformation at 1550 cm^{-1} for amide II.[51] Most of the remaining peaks, at 1040, 1079, 1317, 1346, 1404, and 1453 cm^{-1} can correspond to the stretching of C—O bonds. Furthermore, on close inspection of the lower wave number region of the spectrum, two bands are observed at 2877 and 2940 cm^{-1}, due to aliphatic symmetric and C—H stretching, respectively (The response of C—H bonds is presented by the absorption peaks at 2940 and 2877 cm^{-1}). These results are in agreement with the observation reported by Pawde et al.[20]

The spectra of SA/G hydrogels show peaks at 3265, 1631, 1453, 1408, 1334, 1081, 1028, and 993 cm^{-1}, which indicate O—H stretch, the COO^- (asymmetric), COO^- (symmetric), C—O, C—O—H, respectively, exhibiting strong intermolecular hydrogen bonding.[51,52] Particularly, the intensity of some peaks decreases with increasing of SA (e.g., 1234 cm^{-1}). The adsorption peak, thanks to the stretching of C—O—C ethers coupled with the 1241 and 1119 cm^{-1} of G, shifts to 1234 cm^{-1}. Moreover, the gelatine band related to amides II 1551 cm^{-1} weakens and almost disappears in the SA/G 70/30 sample. The band of SA/G 30/70 at 3291 cm^{-1} shifts to a

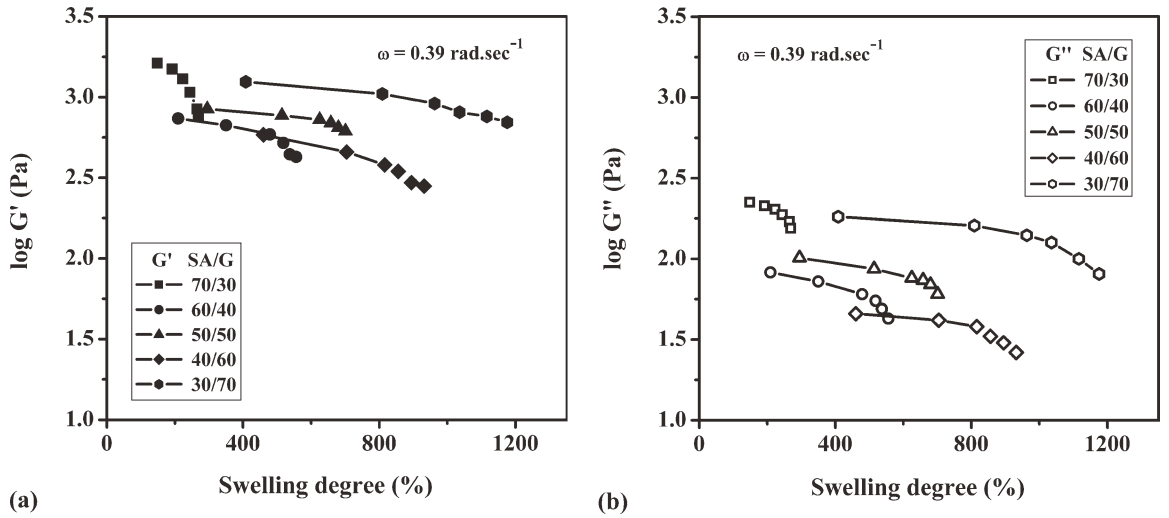

Figure 8 Relation between viscoelastic properties (G' and G'') at angular frequency of 0.39 rad s^{-1} and degree of swelling (%) for samples C.

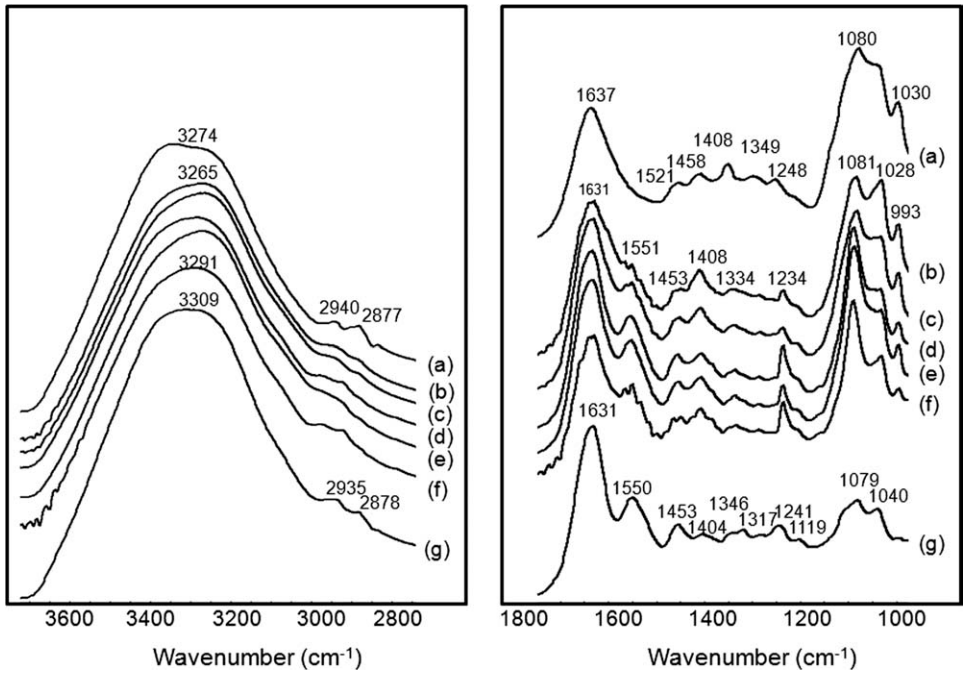

Figure 9 FTIR spectra for: (a) SA/G-100/0, (b) SA/G-70/30, (c) SA/G-60/40, (d) SA/G-50/50, (e) SA/G-40/60, (f) SA/G-30/70, and (g) SA/G-0/100.

lower wavenumber (3265 cm^{-1}) with an increasing concentration of SA which reflects increased hydrogen bonding between SA and G.

CONCLUSIONS

In this work, SA/G hydrogels based on SA and gelatine (G) are introduced as potential wound dressing materials. To evaluate the performance of SA/G hydrogels for wound dressing applications, the morphology, swelling behavior and viscoelastic properties of hydrogels with various ratios of SA and G have been investigated. The results demonstrate that SA/G ratio remarkably influences the structure and morphology of hydrogels. In particular, it is obvious that with a decrease in SA content, the respective hydrogel morphology changes from particle-like to fibrous-like. It can also be observed that the hydrogel morphology closely correlates with the swelling degree, which decreases with an increase in SA content. Results from the determination of water content and swelling behavior show that hydrogels exhibit a high capability to absorb fluid, making them promising materials for exudative wound dressings. The viscoelastic properties of SA/G hydrogels notably depend on their composition and are related to the swelling behavior of hydrogels. The viscoelastic properties of SA/G hydrogels decreased, with an increased swelling degree due to water absorption into the hydrogel structure. The optimum SA/G ratio in terms of a compromise between viscoelastic properties and absorption abilities was found to be SA/G 50/50. The hydrogel with this composition shows the viscoelastic response fully comparable with that of human skin while simultaneously retaining very good absorption properties.

This article was created with support of Operational Program Research and Development for Innovations co-funded by the European Regional Development Fund (ERDF) and national budget of Czech Republic, within the framework of project Centre of Polymer Systems (reg. number: CZ.1.05/2.1.00/03.0111).

References

1. Annie, J.; David V. J Orthop Nurs 2005, 9, 51.
2. Lloyd, L. L.; Kennedy, J. F.; Methacanon, P.; Paterson, M.; Knill, C. J. J Carbohydr Polym 1998, 37, 315.
3. Stephen, T. In The Epidermis in Wound Healing; Rovee, D. T.; Maibach, H. I., Eds.; CRC Press: Washington, DC, 2004, Chapter 12.
4. Boateng, J. S.; Matthews, K. H.; Stevens, H. N.; Gillian. M. Eccleston. J Pharm Sci 2008, 97, 2892.
5. Smith, T. J.; Kennedy, J. E.; Higginbotham, C. L. J Mater Sci Mater Med 2009, 20, 1193.
6. Northern Health and Social Services Board, NHSSB wound management manual, United Kingdom, 2005.
7. Smith, T. J.; Kennedy, J. E.; Higginbotham, C. L. J Mech Behav Biomed Mater 2009, 2, 264.
8. Donati, I.; Paoletti, S. In Alginates: Biology and Applications; Rehm, B. H. A. Ed.; Springer-Verlag: Berlin Heidelberg, 2009, Chapter 1.
9. Immirzi, B.; Santagata, G.; Vox, G.; Schettini, E. J Biosys Eng 2009, 102, 461.

10. Coviello, T.; Matricardi, P.; Marianecci, C.; Alhaique, F. J Control Release 2007, 14, 5.
11. Jong, O. K.; Jung, K. P.; Jeong, H. K.; Sung, G. J.; Chul, S. Y.; Dong, X. L. J Pharm 2008, 359, 79.
12. Thomas, A.; Harding, K. G.; Moore, K. J Biomater 2000, 21, 1797.
13. Paul, W.; Sharma, C. P. In Encyclopedia of Surface and Colloid Science, Marcel Dekker: New York, 2004.
14. Farris, S.; Schaich, K. M.; Liu, L. S.; Piergiovanni, L.; Yam, K. L. J Trends Food Sci Technol 2009, 20, 316.
15. Ioannis S. Arvanitoyannis. In Protein-Based Films and Coatings, Gennadios, A., Ed.; CRC Press: Florida, 2000, Chapter 11.
16. Sperling, L. H. In Introduction to Physical Polymer Science, Sperling, L. H., Ed.; John Wiley & Sons: Canada, 2006, Chapter 9.
17. Schrieber, R.; Gareis, H. Gelatine Handbook; Wiley-VCH: Germany, 2007.
18. Peng, H. T.; Martineau, L.; Shek, P. N. J Mater Sci Mater Med 2008, 19, 997.
19. Zhang, Z. K.; Li, G. Y.; Shi, B. J Soc Leather Technol Chem 2006, 90, 23.
20. Pawde, S. M.; Deshmukh, K. J Polym Sci 2008, 109, 3431.
21. Yoo, H. J.; Kim, H. D. J Pharm 2007, 359, 326.
22. Yakimets, I.; Paes, S. S.; Wellner, N.; Smith, A. C.; Wilson, R. H.; Mitchell, J. R. J Biomacromol 2007, 8, 1710.
23. Slaughter, B. V.; Khurshid, S.; Fisher, O. Z.; Khademhosseini, A.; Peppas, N. A. J Adv Mater 2009, 21, 3307.
24. Cole, S.; Garbe, M. Alginate Hydrogel foam Wound Dressing, US Patent 4,948,575, 1990.
25. Murakami, K.; Aoki, H.; Nakamura, S.; Nakamura, S.; Nakamura, S.; Takikawa, M.; Hanzawa, M.; Kishimoto, S.; Hattori, H.; Tanaka, Y.; Kiyosawa, T.; Sato, Y.; Ishihara, M. J Biomater 2010, 31, 83.
26. Mei, H. H.; Ming, C. Y. J Polym Adv Technol 2009, 4, 1.
27. Chun, M. D.; Lan, Z. H.; Ming, Z.; Dan, Y.; Yi, L. J Carbohydr Polym 2007, 69, 583.
28. Weng, L.; Pan, H.; Chen, W. J Biomed Mater Res A 2007, 2, 352.
29. Choi, Y. S.; Lee, S. B.; Hong, S. R.; Lee, Y. M.; Song, K. W.; Park, M. H. J Mater Med 2001, 12, 67.
30. Balakrishnana, B.; Mohantyb, M.; Umashankarc, P. R.; Jayakrishnana, A. J Biomater 2005, 26, 6335.
31. Mallika, S. K. Imaging Viscoelasticity in Hydropolymers and Breast Tissue Ultrasound, PhD Thesis, University of California, Davis, 2006.
32. Meyvis, T. K. L.; Stubbe, B. G.; Van Steenbergen, M. J.; Hennik, W. E.; De Smedt, S. C. J. Demeester, J. J Pharm 2002, 244, 163.
33. Matthews, K. H.; Auffret, A. D.; Humphrey, M. J.; Stevens, H. N. E.; Eccleston, G. M. J Pharm 2005, 289, 51.
34. Razzak, M. T.; Erizal, Z.; Dewi, S. P.; Lely, H.; Taty, E.; Sukirno, C. J Radiat Phys Chem 1999, 55, 153.
35. Stadler, R.; Gronski, W. J Colloid Polym Sci 1983, 261, 215.
36. Cote, G. L.; Gant, R. M.; Melissa, G.; Yaping, A. H. Self-Cleaning Membrane for Implantable Biosensors: Dynamic mechanical analysis (DMA) and tensile test, US Pat. 20,100,056,894, 2010.
37. Anseth, K. S.; Bowman, C. N.; Brannon-Peppas, L. J Biomater 1996, 17, 1647.
38. Otegui, J.; Fernandez, E.; Retama, J. R.; Cabarcos, E. L.; Mijiangos, C.; Lopez, D. J Polym Eng Sci 2009, 49, 964.
39. Lutz, P. J. J Polym Bull 2007, 58, 161.
40. Denda, M.; Sokable, T.; Fukumi-Tominaga, T.; Tominaga, M. J Invest Dermatol 2007, 127, 654.
41. Bajpai, J.; Mishra, S.; Bajpai, A. K. J Appl Polym Sci 2007, 106, 961.
42. Anmika, R.; Bajpai, J.; Baijai, A. K. J Chem Technol 2009, 16, 388.
43. Agustin, M. R.; Fausto, B. B.; Juan, C.; Sanchez, D.; Alejandro, G. A. J Polym Bull 2009, 62, 539.
44. Mehrdad, K.; Mohammad, S.; Zuhair, M. H. J Eur Polym 2007, 42, 773.
45. Barbara, I.; Gabriella, S.; Giuliano, V.; Evelia, S. J Biosys Eng 2009, 102, 461.
46. Holt, B.; Tripathi, A.; Mordan, J. J Biomech 2008, 28, 2689.
47. Parul, N.; Connie, K. S.; Charles, W. P. J Biomech 2005, 3, 313.
48. Zhanfeng, D.; Qun, W.; Yumin, D. J Membr Sci 2006, 280, 37.
49. Simonida, L. T.; Maja, M. M.; Sava, N. D.; Jovanka, M. F.; Suljovrujic, E. H. J Radiat Phys Chem 2009, 1, 1.
50. Ademar, B. L.; Sizue, O. R.; Sonia, M. M. J Radiat Phys Chem 2002, 63, 543.
51. Lambert, B.; Shurvell, H. F.; Lightner, D.; Cooks, R. G. Organic Structural Spectroscopy; Wiley-VCH: New York, 2007.
52. Barbara, H. S. Infrared Spectroscopy: Fundamentals and applications; Wiley & Sons: England, 2004, Chapter 5.